Organic Chemistry: An Indian Journal

Organic Chemistry
ISSN: 0974-7516

Research | Vol 15 Iss 8

Synthesis of New Heterocycles with a Spiran Junction (Spiro 2-Isoxazoline-γ-Lactone) using the Microwave Oven Technique in a Dry Environment (SiO_2)

Youssef Youssefi[1], Omar Ou-ani[1], Lahcen Oucheikh[1], Abdeslam Ansari[3], Bouchaib Ait Haddou[1,2], Mohamed Znini[1], Mohamed Azrour[1], Ahmad Oubair[1*]

[1]Laboratory Materials Engineering for the Environment and Natural Resources, Faculty of Science and Techniques, Boutalamine, Errachidia, Moulay Ismail University, Meknes, Morocco

[2]Electrochemistry and Environment, Faculty of Sciences, Ibn Tofaïl University, Kenitra, Morocco

[3]Laboratory C.P.A Chemistry: Aggregation Preparation Center: Regional Center for Education and Training Trades, Marrakech SAFI, Morocco

[*]**Corresponding author:** Ahmad Oubair, Laboratory, Materials Engineering for the Environment and Natural Resources, Faculty of Science and Techniques, Boutalamine, Errachidia, Moulay Ismail University, Meknes, Morocco, Tel: 212639647661; E-Mail: oubair-hmad@yahoo.fr

Received: July 12, 2021; **Accepted:** July 19, 2021; **Published:** August 31, 2021

Abstract

The new bicyclic systems with a spiran junction between the two nuclei, 2-isoxazoline and γ-lactone, are obtained by condensation of α-benzylidenyl-γ-butyrolactone and phenylnitroloxide using the microwave oven technique in a dry environment (SiO_2). The structures of these new products are identified using ^1H, ^{13}C NMR and IR spectroscopic analyzes as well as by a radiocrystallographic study by X-ray diffraction on the single crystal of product 3a.

Keywords: ***Spiran junction; α-arylidene-γ-butyrolactone; Spiro 2-isoxazoline-γ-lactone; Microwave oven; X-ray***

Introduction

The biological interest of 2-isoxazoline derivatives and ring-based compounds γ-lactone encouraged us to synthesize new heterocyclic systems with a spiran junction between these two nuclei [1-14]. This synthetic approach was developed in twos tips. The first step consists in preparing the α-benzylidenyl-γ-butyrolactone building blocks and the phenylnitroloxide, while in the second step, we carried out the condensation of the two precursors in the presence of triethylamine (Et3N) using the microwave oven technique in a dry environment (SiO_2), for 12 minutes and under a power of 300W" [15-16]. These spiro adducts are obtained by cycloaddition of the 1,3-dipole formed *in situ* from phenylnitroloxide on the double bond of the α-arylidene-γ-butyrolactone synthon (dipolarophil). The structures of these new compounds were identified using 1H NMR, 13C and IR spectroscopic analyzes. In addition, a structural analysis by X-ray diffraction confirms the proposed structure.

Citation: Youssefi Y, Ou-ani O, Oucheikh L, et al. Synthesis of New Heterocycles with a Spiran Junction (Spiro 2-Isoxazoline-γ-Lactone) using the Microwave Oven Technique in a Dry Environment (SiO_2). Org Chem Ind J. 2021;15(8):32

Experimental Part

Generalities

The source of the microwave is a multimode oven. The emitted waves are not focused and the incident power varies from 100 W to 900 W. Melting points were determined using the Kofler bench. The infrared spectra were recorded using the BRUKER DTGS KBr spectrometer. The 1H and 13C NMR spectra were recorded by the BRUKER AVANCE I apparatus with a frequency of 300 MHz for 1H NMR and 75 MHZ for 13C NMR. Crystallographic data is obtained by the Rigaku Oxford-Diffraction Gemini EOS diffractometer.

General procedure of the preparation of spiro 2-isoxazoline-γ-lactone

In a 250 ml Erlenmeyer flask, mix 3 g (17.24 mml) of α-benzylidenyl-γ-butyrolactone, 2.67 g (17.24 mml) of phenylnitroloxide and 4.86 ml (34.9 mml) of tris ethylamine (Et_3N) dissolved in 5 ml of ethanol and 5 g of natural support. The mixture is activated under microwave irradiation at a power of 300 W for 12 minutes. The organic material is recovered with diethylether, the natural support is removed by filtration and the solvent is evaporated under reduced pressure. The product is purified by chromatography column in silica gel with the eluent (hexane/ethylacetate 80%/20%).

Product identification 3a

White product, m.p=116°C, Yield=85%.

RMN ^{1}H (300 MHz, DMSO), δ (ppm): 3.39 (s, H, $^{4'}CH$); 2.05 (m, 2H, $^{4}CH_2$); 4.31 (m, 2H, $^{5}CH_2$); 7.30-7.66 (m, 10H, $CH_{unsaturated}$).

RMN ^{13}C (75 MHz, DMSO), δ (ppm):18.51(C^4); 55.42 ($^{4'}C$); 65.94 (^{5}C); 88.26 ($^{3.5'}C$); 127.28-127.57-128.26-128.49-128.90-129.18-129.97-130.56-134.51 ($C_{unsaturated}$); 159.85 ($^{3'}C$); 174.05 (C=O).

IR (KBr), (υ in cm^{-1}): $\upsilon_{(C=C)=}$1651; $\upsilon_{(C=O)}$=1732.16; $\upsilon_{(CH\ sp3)}$=2990.4; $\upsilon_{(CH\ sp2)}$=(3018.57-3098.38).

Product identification 3b

White product, m.p=98°C, Yield=80%.

RMN 1H (300 MHz, DMSO), δ (ppm): 2.52 (s, H, $^{4'}CH$); 3.23 (m, 2H, $^{4}CH2$); 4.42 (m, 2H, $^{5}CH2$); 7.30-7.54 (m, 9H, $CH_{unsaturated}$).

RMN ^{13}C (75 MHz, DMSO), δ (ppm): 26.04 (^{4}C); 55.02 ($^{4'}C$); 65.49 (^{5}C); 88.26 ($^{3.5'}C$); 127.28-127.77-128.26-128.49-129.98-129.18-130.54-134.50 ($C_{unsaturated}$); 159.84 ($^{3'}C$); 174.05 (C=O).

IR (KBr), (υ in cm^{-1}): $\upsilon_{(C=O)}$=1736.98; $\upsilon_{(C=C)}$=1650.02; $\upsilon_{(CH\ sp3)}$=2995.32; $\upsilon_{(CH\ sp2)}$ =(3048.44-3085.47).

Product identification 3c

White product, m.p=128°C, Yield=80%.

RMN 1H (300 MHz, DMSO), δ (ppm): 2.52 (s, H, $^{4'}CH$); 3.20 (m, 2H, $4CH_2$); 4.42 (m, 2H, $5CH_2$); 7.03-7.60 (m, 9H, $CH_{unsaturated}$).

RMN 13C (75 MHz, DMSO), δ (ppm): 26.80 (^{4}C); 56.02 ($^{4'}C$); 65.29 (^{5}C); 88.26 ($^{3.5'}C$); 114.42-121.93-127.11-131.41-131.80-132.19-134.54 ($C_{unsaturated}$); 160.39 ($^{3'}C$); 172.16 (C=O).

IR (KBr), (υ in cm^{-1}): $\upsilon_{(C=C)}$=1649.82; $\upsilon_{(C=O)}$=1737.07; $\upsilon_{(CH\ sp3)}$=2928.57; $\upsilon_{(CH\ sp2)}$=(3048.42-3088.39).

Product identification 3'a

White product, m.p=110°C, Yield=8%. RMN 1H (300 MHz, DMSO), δ (ppm): 2.05 (m, 2H, $^{4}CH_2$); 4.42 (m, 2H, $^{5}CH_2$); 5.29 (s, H, $^{4'}CH$); 7.03-7.66 (m, 10H, $CH_{unsaturated}$).

RMN 13C (75 MHz, DMSO), δ (ppm): 29.04 (^{4}C); 65.94 ($^{4'}$C); 65.29 (^{5}C); 55.02 ($^{3,5'}$C); 127.2-127.77-128.26-128.49-128.89-129.18-130.54-134.50 ($C_{unsaturated}$); 159.84 ($^{3'}$C); 174.05 (C=O).

IR (KBr), (υ in cm^{-1}): $\upsilon_{(C=C)}$=1651; $\upsilon_{(C=O)}$=1732.16; $\upsilon_{(CH\ sp^3)}$ =2990.4; $\upsilon_{(CH\ sp^2)}$=(3018.57-3098.38) **SCHEME 1.**

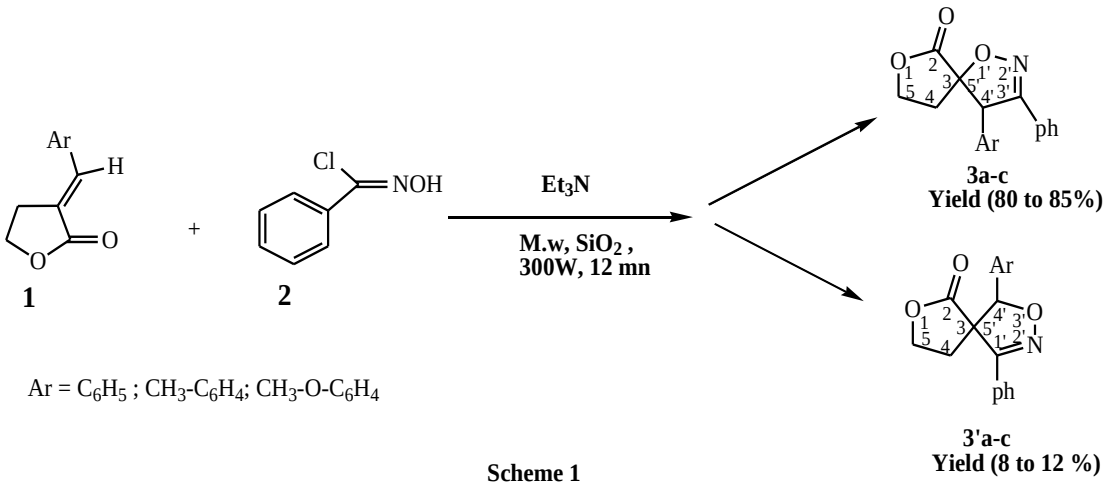

Scheme 1

SCHEME. 1. **Synthesis route of the compounds 3a-c and 3'a-c.**

Results and Discussion

The dipolar-1,3 cycloaddition in volves four electrons from the dipole and two electrons from the dipolarophile. During the reaction, the dipole and dipolarophile approach in two substantially parallel planes to lead, after hybridization of the system and formation of two new σ bonds, to a pentagonal heterocycle. The essential consequence of this concerted condensation is the cis steriospecificity of the cycloaddition reactions and that the dipole has the possibility of adding on both sides of the double bond of the dipolarophil. This cycloaddition of the 1,3-dipole formed in situ from the phenylnitroloxide can have two directions of addition on the benzylidene unit, one for which the quaternary carbon of the spiran junction is linked to the oxygen 3a-c**,** the other which places in α of the quaternary carbon a hybridized carbon $sp^2$3'a-c. The products of the 3a-3c series are obtained with good yields ranging from 80% to 85% while those of the 3'a-c series vary between 8% to 12%. Besides these adducts, we have also isolated secondary products which maybe the dimmers originating from the 1,3-dipole formed in situ according to the literature but with low returns that do not exceed 2%. Optimizing yields and contributing to environmental protection by reducing the use of organic solvents and the formation of residues (side reactions) remains the essential dependency of the operating protocol employed [17]. These considerations sled us to deploy the microwave oven technique in a dry environment (SiO_2).

The structures of the new heterocycles are identified using spectral analyzes. According to the H NMR spectra of the 3a-c products, one notices the conservation of the skeleton of the γ-lactone nucleus of the starting precursor of which these two methine groups $4CH_2$ and $5CH_2$ appear respectively at (2.053 ppm and 4.318 ppm), (3.23 ppm and 4.42 ppm) and (3.30 ppm and 4.41 ppm). Thus, these spectroscopic analyzes show the transformation of the benzylidene unit which has undergone the cycloaddition of the 1,3-dipole and the creation of two asymmetric carbons ($C^{4'}$, $C^{3.5'}$) which already gives optical activity to the new compounds and the C4' carbon proton resonate at 2.50 ppm, 2.52 ppm and 2.52 ppm respectively in the strong field zone. The presence of these two C4' and $C^{3,5'}$ is confirmed by the ^{13}C NMR spectrum, of which the chemical shift of the spiran

junction carbon $C^{3,5'}$ is respectively of the order of 88.263 ppm, 88.26 ppm and 88.26 ppm which is strongly reined. By its bond to an oxygen atom and to a carbonyl while the peak of the C4′ carbon appears at 55.428 ppm, 56.02 ppm and 56.03 ppm respectively [18]. While for the other 3'a-c diastereisomers and according to the analysis of the H NMR spectral of compound 3'a, we find that the proton of $C^{4'}$appears in the form of a peak at 5.29 ppm because of its binding to oxygen which makes it more de-shielded and the ^{13}C NMR spectrum shows that the two quaternary carbons $C^{4'}$ and $C^{3.5'}$ appear at 65.31 ppm and 55.02 ppm respectively. These analyses are in accordance with the proposed structures. In order to confirm the proposed structures, we have recourse to a radiocrystallographic study by X-ray diffraction on the single crystal of product 3a **(FIG. 1)** [18].

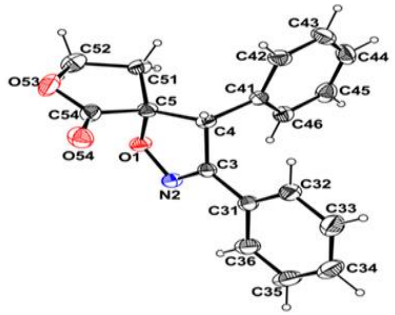

FIG. 1. **Structure of compound 3a**.

^{1}H NMR, ^{13}C NMR and IR spectroscopic study of product 3a-c

1H NMR spectra reveal: Signals of aromatic protons which appear as a clump between (7.30 ppm-7.66 ppm), (7.30 ppm-7.54 ppm) and (7.03 ppm-7.60 ppm) respectively. Two massifs centered at (2.05 ppm and 4.31 ppm), (3.23 ppm and 4.42 ppm) and (3.20 ppm and 4.42 ppm) characterizing the protons of the C^4 and C^5 carbons. The $C^{4'}$ carbon proton appears as a singlet at 3.39 ppm, 2.52 ppm and 2.52 ppm respectively.

The ^{13}C NMR spectra show the appearance of the peak corresponding to the carbonyl group (C=O) around 172.166 ppm, 174.05 ppm and 174.05 ppm respectively. The peak corresponding to the spiran junction carbon $C^{3.5'}$appears at around 88.26 ppm, 88.26 ppm and 88.26 ppm. The peak of $C^{4'}$carbon is observed at 55.42 ppm, 56.02 ppm and 56.02 ppm respectively in the region of the sp^3 hybridized carbons. The peaks of the two carbons C^4 and C^5 are revealed respectively at (18.51 ppm, 65.94 ppm), (26.04 ppm, 65.49 ppm) and (26.80 ppm, 65.29 ppm). The peaks of the other unsaturated carbons (hybridized sp^2) of the phenyl appear between (127.28 ppm-159.85 ppm), (127.28 ppm, 159.84 ppm) and (114.40 ppm, 160.37 ppm) respectively.

The IR spectra of the 3a-c products make it possible to identify in particular an intense absorption band characteristic of the carbonyl group which appears respectively at 1732.16 cm^{-1}, 1736.98 cm^{-1} and 1737.07 cm^{-1}.

^{1}H NMR, ^{13}C NMR and IR spectroscopic study of product 3'a

^{1}H NMR spectra reveal: Signals of aromatic protons which appear as a clump between (7.30 ppm-7.66 ppm). Two massifs centered at 2.05 ppm and 4.31 ppm characterizing the protons of the C^4 and C^5 carbons. The carbon C4' proton appears as a singlet at 5.29 ppm.

The ^{13}C NMR spectra show the appearance of the peak corresponding to the carbonyl group (C=O) at around 174.05 ppm. The peak corresponding to the spiran junction carbon $C^{3.5'}$ appears at 55.02 ppm. The peak of C^4 carbon is observed at 61.31

ppm. The peaks of the two carbons C^4 and C^5 are revealed at 29.04 ppm 65.94 ppm. The peaks of the other unsaturated carbons (hybridized sp^2) of the phenyls appear between (127.28 ppm and 159.84 ppm).

The IR spectrum confirms the presence of the carbonyl group in the structure whose band appears at 1737.07 cm^{-1}.

X-ray structural analyses

A single crystal of compound 3a was mounted under inert perfluoropolyether on the tip of a glass fibre and cooled in the crystream of a Rigaku Oxford-Diffraction Gemini EOS diffractometer. The structure was solved by using the integrate space-group and crystal structure determination SHELXT software and refined by least-squares procedures on F^2 using SHELXL-2014 [19,20]. All H atoms attached to carbon were introduced in calculation in idealised positions and treated as riding models. The crystal and refinement parameters are collected in (**TABLE 1**) and the full list of bond distances and angles provided in **(TABLE 2).** The drawing of the molecules was realised with the help of ORTEP32 [21,22] and MERCURY [23]. Atomic coordinates and thermal anisotropic parameters are given in **TABLES 3** and **4**. The crystal and refinement parameters are collected in **(TABLE 1).**

TABLE 1. **Crystal data.**

Identification code	**3a**
Empirical formula	$C_{18}\ H_{15}\ N\ O_3$
Formula weight	293.31
Temperature, K	173 (2)
Wavelength, Å	1.54184
Crystal system	Orthorhombic
Space group	P b c a
a, Å	9.1273 (2)
b, Å	10.1696 (2)
c, Å	30.6331 (7)
Volume, Å3	2843.40 (11)
Z	8
Density (calc), Mg/m^3	1.37
Abs. coefficient, mm^{-1}	0.763
F (000)	1232
Crystal size, mm^3	0.370 × 0.250 × 0.080
Theta range°	5.643 to 61.610
Reflections collected	7329
Indpt reflections (R_{int})	2212 (0.0240)
Completeness, %	100
Absorption correction	Multi-scan
Max. and min. transmission	1.0/0.5645
Refinement method	Full-matrix on F2
Data /restraints/parameters	2212/0/199
Goodness-of-fit on F2	1.047
R1, wR2 (I>2s (I)	0.0334, 0.0827
R1, wR2 (all data)	0.0368, 0.0853
Residual density, e.Å-3	0.170/-0.203

TABLE 2. **Bond distances (Å) and bond angles (°) for compound 3a.**

Bonds	**Bond distance (°)**	**Bonds**	**Bond distance (°)**
O(1)-C(5)	1.4626 (16)	O(1)-N(2)	1.4248 (15)
O(53)-C(54)	1.3414 (19)	N(2)-C(3) 1.2839(17)	1.2839 (17)
O(54)-C(54)	1.2009 (18)	O(53)-C(52) 1.457(2)	1.457 (2)
-	-	C(52) C(51) 1.518(2)	1.518 (2)
C(3)-C(31)	1.4702 (19)	C(3)-C(4) 1.5139(18)	1.5139 (18)
C(4)-C(41)	1.5208 (18)	C(4)-C(5) 1.5296(18)	1.5296 (18)
C(5)-C(54)	1.5322 (19)	C(5)-C(51) 1.5107(19)	1.5107 (19)
C(33)-C(34)	1.380 (2)	C(31)-C(32) 1.388(2)	1.388 (2)
C(34)-C(35)	1.384 (2)	C(31)-C(36) 1.399(2)	1.399 (2)
C(35)-C(36)	1.377 (2)	C(32)-C(33) 1.392(2)	1.392 (2)
C(43)-C(44)	1.384 (2)	C(41)-C(42) 1.391(2)	1.391 (2)
C(44)-C(45)	1.378 (2)	C(41)-C(46) 1.392(2)	1.392 (2)
C(45)-C(46)	1.387 (2)	C(42)-C(43) 1.384(2)	1.384 (2)
Type of Bonds	**Bond angle (°)**	**Type of Bonds**	**Bond angle (°)**
N(2)-O(1)-C(5)	107.58 (9)	N(2)-C(3)-C(31) 120.40(12)	120.40 (12)
C(54)-O(53)-C(52)	110.39 (11)	N(2)-C(3)-C(4) 113.67(11)	113.67 (11)
C(3)-N(2)-O(1)	109.08 (10)	C(3)-C(4)-C(41) 111.97(10)	111.97 (10)
C(3)-C(4)-C(5)	99.05 (10)	C(41)-C(4)-C(5) 113.03(10)	113.03 (10)
C(31)-C(3)-C(4)	125.77 (12)	O(53)-C(52)-C(51) 105.17(12)	105.17 (12)
O(1)-C(5)-C(51)	109.56 (11)	O(54)-C(54)-O(53) 122.55(13)	122.55 (13)
O(1)-C(5)-C(4)	104.04 (10)	O(54)-C(54)-C(5) 128.02(13)	128.02 (13)
C(5)-C(51)-C(52)	102.37 (12)	O(53)-C(54)-C(5) 109.42(12)	109.42 (12)
C(51)-C(5)-C(4)	120.89 (11)	C(51)-C(5)-C(54) 102.58(11)	102.58 (11)
O(1)-C(5)-C(54)	104.45 (10)	C(4)-C(5)-C(54) 114.27(11)	114.27 (11)
C(32)-C(31)-C(36)	118.97 (13)	C(36)-C(35)-C(34) 120.48(14)	120.48 (14)
C(32)-C(31)-C(3)	120.68 (12)	C(36)-C(31)-C(3) 120.36(13)	120.36 (13)
C(31)-C(32)-C(33)	120.34 (14)	C(34)-C(33)-C(32) 120.05(15)	120.05 (15)
C(33)-C(34)-C(35)	119.87 (14)	C(35)-C(36)-C(31) 120.30(15)	120.30 (15)
C(42)-C(41)-C(46)	118.89 (13)	C(44)-C(45)-C(46) 120.09(14)	120.09 (14)
C(42)-C(41)-C(4)	120.09 (12)	C(46)-C(41)-C(4) 120.88(12)	120.88 (12)
C(43)-C(42)-C(41)	120.28 (14)	C(45)-C(44)-C(43) 119.79(14)	119.79 (14)
C(44)-C(43)-C(42)	120.40 (14)	C(45)-C(46)-C(41) 120.54(14)	120.54 (14)

TABLE 3**. Hydrogen-bond geometry (Å, º) for 3a.**

D-H	D-H···A	H···A	D···A	D-H···A
1	C4-H4···O1^{i}	2.49	3.4194 (16)	154
0.99	C51-H51A···O54^{ii}	2.5	3.4834 (18)	171
Symmetry codes: (i): -x+3/2, y-1/2, z; (ii): -x+3/2, y+1/2, z				

Structural Description

As expected, the structure of compound 3a is built up by the association of a butyrolactone and an oxazole rings linked through a spiro carbon (**FIG. 1).** The oxazole ring is further substitued by two phenyl rings. These phenyl rings make a dihedral angle close to 90° with a value of 88.39 (5°). The two five membered rings display envelope conformation with puckering parameters Q2=0.249 and ϕ=-318° for the oxazole ring and Q2=0.311 and ϕ=73° for the butyrolactone ring **(FIG. 2**) [24, 25].

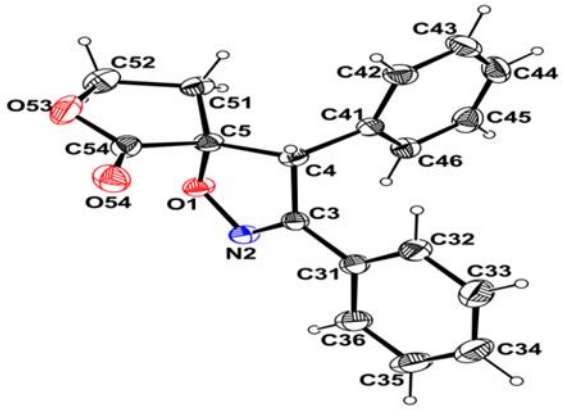

FIG. 2**. Molecular view of compound 3a with the atom labelling scheme. Ellipsoids are drawn at the 50% probability level. H atoms are represented as small spheres of arbitrary radii.**

The packing is stabilized by C-H•••O and C-H•••N hydrogen bonds. The C44-H44•••N2 (-1+x, y, z) built up a linear C (8) chains parallel to the a axis (**TABLE 3, FIG. 2**). These chains are linked by C-H•••O hydrogen bonds (C4-H4-O1(-x+3/2, y-1/2)) and (C51-H51A•••O54 (-x+3/2, y+1/2, z)) building up a R22 (9) graph set motif (**FIG. 3**) leading to the formation of a two dimensional network parallel to the (0 0 1) plane **FIG. 4** [26]**.** Partial packing view showing the formation of the two dimensional network **(FIG. 5**).

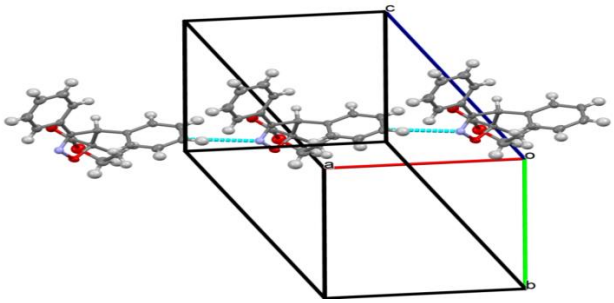

FIG. 3. **Partial packing view showing the formation of the C8 chain through the C-H...N interactions.**

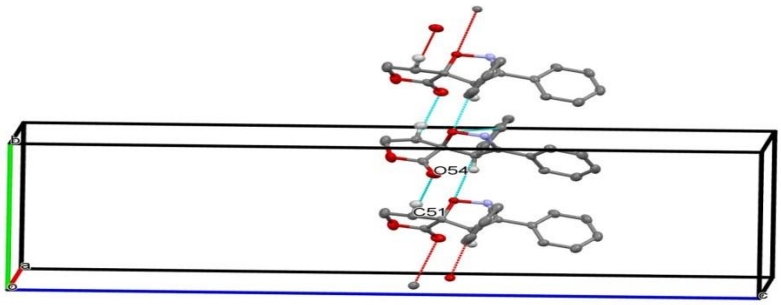

FIG. 4. **Partial packing view showing the formation of the R22 (9) rings through the C-H...O interactions.**

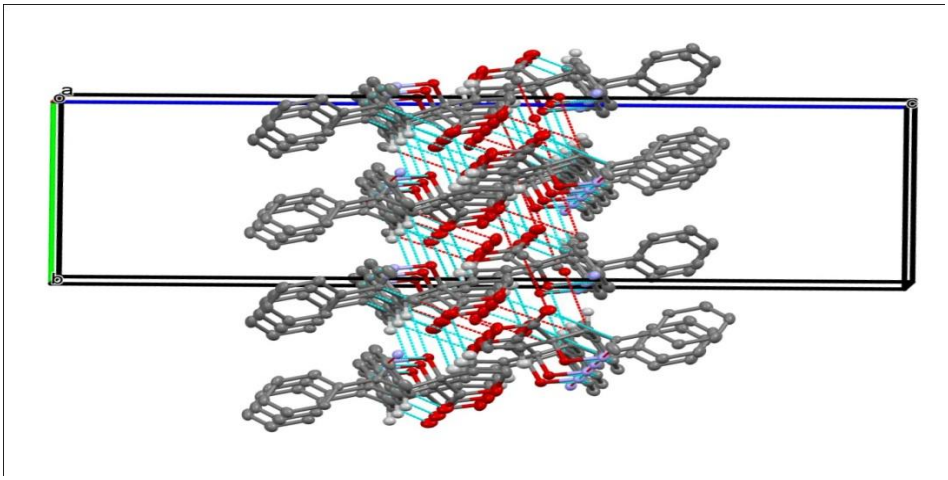

FIG. 5. **Partial packing view showing the formation of the two dimensional network.**

A search in the Cambridge Structural Database using the fragment built up by a spiro carbon connecting butyrolactone and oxazole five membered rings reveals 6 hits [27]. A comparison of selected bond distances and bond angles within the spiro fragment for compound 1 and related structure in the literature shows that the geometry is not really affected by the nature of the substituent on the hetrocyclic five membered rings (**TABLE 4 and TABLE 5**).

TABLE 4. **Comparison of selected bond distances and bond angles between compound 3a and related spiro structures [28-32].**

S No.	C5-O1	C5-C54	C5-C51	C5-C4	O1-N2	N2-C3	C54-O53	C54-O54
1	1.463 (2)	1.533 (2)	1.510 (2)	1.530 (2)	1.425 (2)	1.284 (2)	1.341 (2)	1.201 (2)
2	1.434	1.653	1.497	1.458	1.44	1.236	1.321	1.277
3	1.433	1.533	1.517	1.535	1.485	1.466	1.332	1.193
4	1.435	1.534	1.514	1.514	1.464	1.488	1.335	1.194
5	1.48	1.529	1.504	1.512	1.438	1.465	1.337	1.185
6	1.466	1.525	1.51	1.53	1.423	1.278	1.348	1.198

7	1.468	1.53	1.507	1.51	1.417	1.281	1.336	1.197

TABLE 5. **Comparison of selected bond distances and bond angles between compound 3a and related spiro structures [28-32].**

S No.	C54-C5-O1	C54-C5-C4	C54-C5-C51	O1-C5-C4	O1-C5-C51	C51-C5-C4
1	104.03 (10)	114.27 (11)	102.58 (11)	104.03 (10)	109.58 (11)	120.9
2	106,56	119.8	107.57	104.19	115.61	103.59
3	108.94	113.19	101.43	104	115.53	114
4	104.08	115.79	102.94	103.44	111.98	118
5	106.2	115.14	102.71	104.54	107.37	120.01
6	105.58	114.16	101.25	104.29	108.77	121.82
7	103.96	114.02	103.2	104.45	110.18	120.03

Conclusion

In this work, we have synthesized new bicyclic compounds with a spiran junction between the two nuclei γ-lactone and 2-isoxazoline. They are obtained by cycloaddition of the 1,3-dipole formed in situ from phenyl nitroloxide on α-arylidene-γ-butyrolactone. These products are synthesized with good yields using the microwave oven technique in a dry environment (SiO2) as an ecological synthesis method. Activation of reactions under microwave irradiation has proven to be highly effective.

The structures of the products obtained ^{1}H NMR and ^{13}C NMR spectroscopic analyzes and fully characterized by X-ray diffraction analyzes. The bicycle formed is likely to exhibit very interesting biological properties.

REFERENCES

1. Dallanoce C, Frigerio F, Martelli G, et al. Novel tricyclic Δ2-isoxazoline and 3-oxo-2-methyl-isoxazolidine derivatives: Synthesis and binding affinity at neuronal nicotinic acetylcholine receptor subtypes. Bioorg Med Chem. 2010;18:4498-508.
2. Kaur K, Kumar V, Sharma AK, et al. Isoxazoline containing natural products as anticancer agents: A review Eur J Med Chem. 2014;77:121-33.
3. Prajapti SK, Shrivastava S, Bihade U, et al. Synthesis and biological evaluation of novel Δ 2-isoxazoline fused cyclopentane derivatives as potential antimicrobial and anticancer agents. Med Chem Comm. 2015;6:839-45.
4. Abolhasani H, Dastmalchi S, Hamzeh Mivehroud M, et al. Design, synthesis and biological evaluation of new tricyclic spiroisoxazoline derivatives as selective COX-$_2$ inhibitors and study of their COX-$_2$ binding modes *via* docking studies. Med Chem Res. 2016;25:858-69.
5. Suresh G, Venkata Nadh R, Srinivasu N, et al. Novel coumarin isoxazoline derivatives: Synthesis and study of antibacterial activities. Synth Commun. 2016;46:1972-80.
6. Ibrahimi S, Sauvé G, Yelle J, et al. Racemic and enantioselective synthesis of enol-lactones and their evaluation as inhibitors of HIV-1 protease. Chem Rep. 2005;8: 75-83.

7. Amtul Z, Follmer C, Mahboob S, et al. Germa-γ-lactones as novel inhibitors of bacterial urease activity. Biochem Biophys Res Commun. 2007;356:457-63.
8. Şardan M, Sezer S, Günel A, et al., Synthesis and biological evaluation of optically active conjugated γ-and δ-lactone derivatives. Bioorg Med Chem Lett. 2012;22:5814-8.
9. Leśniak A, Smuga M, Białońska A, et al. Lactones 44. Microbial lactonization of γ-ketoacids. J Mol Catal B: Enzym. 2014;106:32-9.
10. Liu YP, Hu S, Wen Q, et al. Novel γ-lactone derivatives from Trigonostemon heterophyllus with their potential antiproliferative activities. Bioorg Chem. 2018;79:107-10.
11. Ebrahimi F, Mahmoudi J, Torbati M, et al. Hemostatic activity of aqueous extract of *Myrtus communis* L. leaf in topical formulation: *in vivo* and *in vitro* evaluations. J Ethnopharmacol. 2020;249:112398.
12. Akca UK, Kesici S, Ozsurekci Y, et al. Kawasaki-like disease in children with COVID-19. Rheumatol Int. 2020:1-1.
13. Fábian M, Gonda J, Jacková D, et al. Synthesis and *in vitro* cytotoxic evaluation of spiro-β-lactone-γ-lactam scaffolds. Tetrahedron. 2020;76:131144.
14. Xu B, Ng TC, Huang S, et al. Evaluation and comparison of the microbial consortia enriched by gamma-caprolactone and N-Acyl homoserine lactones for effective quorum sensing disruption. Int Biodeterior Biodegrad. 2021;159:105200.
15. Oubair A, Fihi R. Synthesis of new derivatives pyridazinones assisted by Microwave on dry medium comparing it to conventional heating. Int J Innov Appl Stud. 2016; 18: 381.
16. Syassi B, Bougrin K, Soufiaoui M. Dipolar-1, 3 Addition of Arylnitriloxides with some Olefinic Dipolarophiles on Alumina in Dry Medium and under Microwaves. Tetrahedron lett. 1997; 38: 8855-8
17. Grundmann C, Frommeld HD. Nitrile Oxides. VIII. Cyanogen N-Oxide[1]. J Org Chem. 1966;31:4235-7.
18. Luck WA. Structure of water and aqueous solutions. Verlag Chemie; 1974.
19. Sheldrick GM. Crystal structure refinement with SHELXL. Acta Crystallographica Section C: Struct Chem. 2015;71:3-8.
20. Sheldrick GM. A short history of SHELX. Acta Crystallographica Section A: Found Crystallogr. 2008 ;64:112-22.
21. Farrugia LJ. ORTEP-3 for Windows-a version of ORTEP-III with a Graphical User Interface (GUI). J Appl Crystallogr. 1997;30:565.
22. Spek AL. Single-crystal structure validation with the program PLATON. J Appl Crystallogr. 2003;36:7-13.
23. Macrae CF, Edgington PR, McCabe P, et al. Mercury: Visualization and analysis of crystal structures. J Appl Crystallogr. 2006;39:453-7.
24. Cremer DT, Pople JA. General definition of ring puckering coordinates. J Am Chem Soc. 1975;97:1354-8.
25. Boessenkool IK, Boeyens JC. Identification of the conformational type of seven-membered rings. J Cryst Mol Struct. 1980;10:11-8.
26. Etter MC. Encoding and decoding hydrogen-bond patterns of organic compound. J Cryst Mol Struct. 1990;23:120-6.
27. Groom CR, Bruno IJ, Lightfoot MP, et al. The Cambridge structural database. Acta Crystallogr. B: Struct Sci Cryst Eng Mater. 2016;72:171-179.
28. Štverková S, Žák Z, Jonas J, et al. 1, 3-Dipolar cycloaddition of benzonitrile oxide to substituted 4, 5-Dihydro-3-methylene-2 (3H)-furanones. Liebigs Annalen der Chemie. 1993;12:1169-73.

29. Cacciarini M, Cordero FM, Faggi C, et al. Cycloaddition Reactions of C, N-Diphenylnitrone to Methylene-γ-butyrolactones. Molecules. 2000;5:637-47.
30. Roussel C, Ciamala K, Vebrel J, et al. Reactivity of arylnitrile oxides and C-aroyl-N-phenylnitrones with 3-methylenedihydro-(3H)-furan-2-one and itaconic anhydride. Heterocycles. 2009;78:1977-91.
31. Li XF, Feng YQ, Xu M, et al. 4-(4-Chlorophenyl)-3-(2, 6-dichlorophenyl)-1, 7-dioxa-2-azaspiro (4.4) non-2-en-6-one. Acta Crystallographica Section E: Structure Reports Online. 2003; 59:o675-6.
32. Štverková S, Žák Z, Jonas J, et al. 1, 3-dipolar cycloaddition of diphenylnitrilimine to substituted dihydro-3-methylene-2 (3H)-furanones. Liebigs Annalen. 1995;3:477-80.